Electron-electron repulsion in carbazole oligomer-attached tris (2,4,6-trichlorophenyl) methyl radicals

Matsuda, Kenshiro
Interdisciplinary Graduate School of Engineering Sciences, Kyushu University

Ota, Wataru
Fukui Institute for Fundamental Chemistry, Kyoto University

Yamaoka, Keiko
Institute for Materials Chemistry and Engineering, Kyushu University

Anraku, Kosuke
Interdisciplinary Graduate School of Engineering Sciences, Kyushu University

他

出版情報：The Journal of Chemical Physics. 162 (16), pp.164305-, 2025-04-22. AIP Publishing
バージョン：

Electron-electron repulsion in carbazole oligomer-attached *tris* (2,4,6-trichlorophenyl) methyl radicals

Kenshiro Matsuda, [a] Wataru Ota, [b, c] Keiko Yamaoka, [d] Kosuke Anraku, [a] Emiko Fujiwara, [b] Kazuhiro Nakamura, [a] Takuya Hosokai, [*e] Tohru Sato, [*b, c] and Ken Albrecht [*d]

a. Interdisciplinary Graduate School of Engineering Sciences, Kyushu University, 6-1 Kasuga-Koen, Kasuga-shi Fukuoka 816-8580, Japan.

b. Fukui Institute for Fundamental Chemistry, Kyoto University, Takano Nishibiraki-cho 34-4, Sakyo-ku, Kyoto, 606-8103, Japan.

c. Department of Molecular Engineering, Graduate School of Engineering, Kyoto University, Nishikyo-ku, Kyoto 615-8510, Japan

d. Institute for Materials Chemistry and Engineering, Kyushu University, 6-1 Kasuga-Koen Kasuga-shi, Fukuoka 816-8580, Japan.

e. National Metrology Institute of Japan (NMIJ), National Institute of Advanced Industrial Science and Technology (AIST), Tsukuba Central 5, 1-1-1 Higashi, Tsukuba, Ibaraki 305-8565, Japan.

E-mail: Ken albrecht albrecht@cm.kyushu-u.ac.jp, Takuya Hosokai, t.hosokai@aist.go.jp, and Tohru sato tsato@scl.kyoto-u.ac.jp

Abstaract

Luminescent radicals are gathering much attention as a new class of luminescent material. We have synthesized a new carbazole oligomer (mono, di, tri, tetra) substituted luminescent *tris* (2,4,6-trichlorophenyl) methyl (TTM) radicals. The photoluminescence (PL) spectra showed emission stemmed from the excited state charge transfer (CT) character. Despite the increase of the HOMO level of the carbazole oligomer associated with increasing the oligomer length, the PL maxima showed a blue shift from di- to tetra-oligomer substitution. This unexpected behavior was explained by quantum chemical calculations, including electron-electron repulsion. The electron-electron repulsion on the donor orbital decreases when the oligomer length increases and leads to the blue shift of the emission. The blue shift of the emission accompanied by an increase in the photoluminescence quantum yield by substituting a large π-conjugated donor to a TTM radical would be a unique method to control the photophysical property of the luminescent radical.

Main text

I. INTRODUCTION

Organic luminescent radicals are open-shell luminescent molecules with unpaired electrons that emit a photon without a spin-flip process accompanying an electronic transition from the lowest doublet excited state (D_1) to the ground doublet excited state (D_0). They can theoretically form 100% doublet excitons through electrical excitation, show no heavy atom effects [1, 2, 3] and have efficient near-infrared luminescence.[4, 5, 6, 7] The spin-originated properties of luminescent radicals[8, 9] make them attractive for applications such as bioimaging,[10, 11] magnetoluminescence,[12, 13, 14] and organic light-emitting diodes (OLEDs).[15] Thus, both understanding the behavior and manipulating the properties of luminescent radicals are important issues for pushing the field of luminescent radicals further.

Perchloro-triphenylmethyl (PTM) [16] and tris(2,4,6-trichlorophenyl)methyl (TTM) [17] the representative organic luminescent radicals, are known to be stabilized by steric protection of the spin by chlorine atoms and delocalization of the spin to the π-conjugated skeleton. The TTM radical has a photoluminescence quantum yield (PLQY) of 2-3% and a half-life under light irradiation of approximately 50 s in cyclohexane. [18, 19] The alternatively symmetric PTM and TTM radicals have a singly occupied molecular orbital (SOMO) between the highest occupied molecular orbital (HOMO) and the lowest unoccupied molecular orbital (LUMO), which weakens the transition dipole moments in HOMO-SOMO and SOMO-LUMO, resulting in D_0-D_1 transitions of minimum oscillator strength.

Donor-acceptor (D-A) luminescent radicals, such as carbazole donor-coupled TTM radicals, are known to increase PLQY and improve photostability by breaking the degeneracy of TTM through disruption of orbital symmetry. This results in D_0-D_1 transition being more permissible and bypassing the local transition of the TTM. While some systematic understanding of the enhanced stability and

highly efficient luminescence of luminescent radicals has been reported, [20, 21, 22, 23] they are not fully understood and further understanding is required.

We have recently reported a luminescent TTM radical coupled to carbazole dendrons (FIG. 1).[24] Carbazole dendrons have a dendritic structure with a potential gradient where the outer layer is electron-rich and the inner layer is electron-poor originated from the summation of the dipole moment of carbazoles. With increasing the generation of the dendron, the HOMO level of the dendron becomes shallower due to the increase in π-conjugation and higher electron density of the outer carbazole.[25] The carbazole dendron attached TTM radicals exhibited an unexpected blue shift in absorption and emission spectra with increasing the generation despite the decrease in the energy gap between the TTM SOMO and the carbazole dendron HOMO obtained by theoretical calculations. More advanced theoretical calculations revealed that the shift stems from a decrease in electron-electron repulsion in occupied orbitals on the π-conjugated dendron fragment with increasing generation. The electron-electron repulsion is another factor than HOMO level to control the CT character, but the generality of the concept should be proven in other luminescent radical molecules.

To explore the effect of electron-electron repulsion, here we designed carbazole oligomer-attached TTM radicals and studied their physical properties and photostability. Carbazole oligomers are fragments of carbazole dendrons and have a well-defined and homogeneous structure similar to the carbazole dendrimers. The HOMO level of carbazole oligomers increases slightly when the oligomer length increases, despite the large torsion between carbazoles weakening the effect of the π-conjugate extension.[26, 27, 28, 29, 30, 31, 32] Thus, we expected that carbazole oligomer-attached TTM radicals show electronic properties different from carbazole-dendronized TTM radicals and would be a good example to deepen the knowledge of the effect of electron-electron repulsion in luminescent radical systems.

FIG. 1

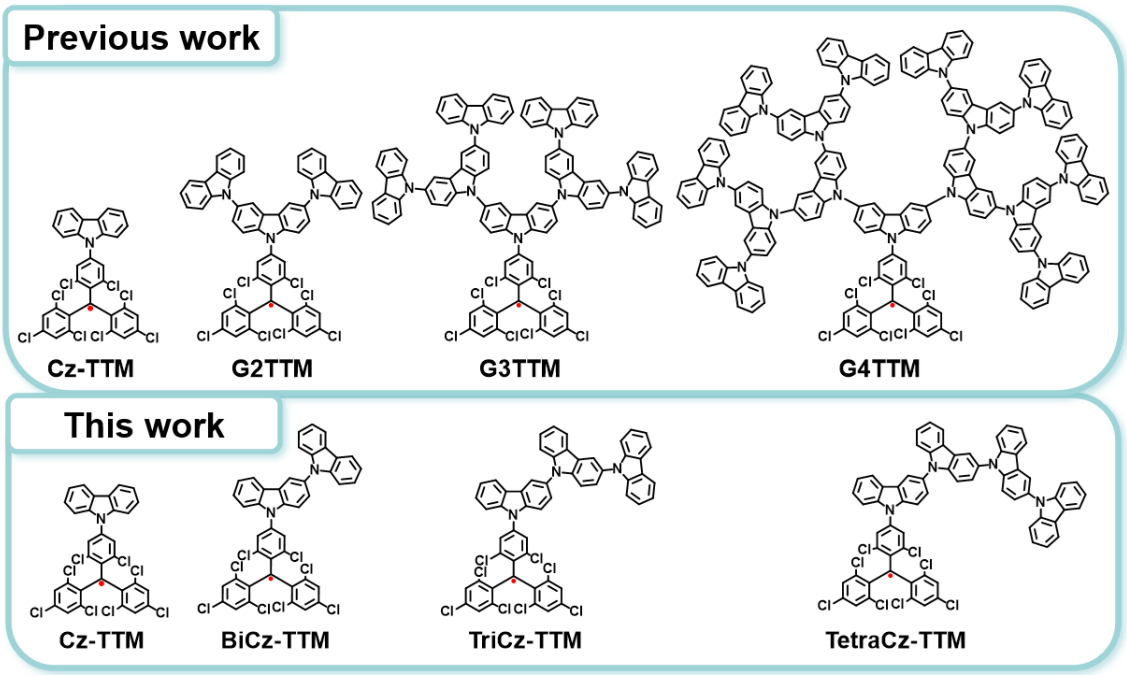

Structure of carbazole oligomer- and dendron-attached TTM radicals.[24]

II. RESULTS AND DISCUSSION

Carbazole oligomer-attached TTM radicals were synthesized according to the previous strategy (detailed synthetic procedures and structural properties are described in the Supporting Information).[22, 25, 33] Carbazole oligomer-attached TTM radical precursors were prepared through a nucleophilic substitution between TTM radicals and oligomeric carbazoles, and the precursors were converted to radical species by treatment with KO*t*Bu and *p*-chloranil, and then isolated and purified using silica gel column chromatography. The radical precursors were characterized by ^{1}H NMR spectra, ^{13}C NMR spectra, MALDI-TOF-MS, and elemental analysis. The new radicals were characterized by MALDI-TOF-MS and elemental analysis, and the presence of unpaired electrons was confirmed using electron spin resonance (ESR) spectroscopy. The purity of the radicals was determined using ^{1}H NMR to confirm the absence of radical precursors, and by comparing the ESR signal intensity with a reference (TEMPOL). The purity was determined to be over 95%. A series of oligomer-attached TTM radical was successfully synthesized.

UV-Vis absorption spectra of the radicals were recorded in toluene for comparison with previously reported carbazole dendronized radicals[24] (Table I, and FIG. 2). All radicals exhibited an absorption band at 374 nm attributed to the π-π* transition of the TTM radical moiety. The absorption bands at longer wavelengths are attributed to charge transfer (CT) transitions from carbazole to TTM and are located at 609 nm (Cz-TTM), 612 nm (BiCz-TTM), 605 nm (TriCz-TTM), and 603 nm (TetraCz-

TTM) (see also Fig. S14). Increasing the oligomer length resulted in a blue shift in absorption, which was observed in various solvents (Figs. S15-S18). Previous studies in the dendronized radicals showed the same behavior.[24] This behavior here can also be explained by the electron-electron repulsion of the carbazole unit, and the details are discussed later in the calculations section. Increasing the oligomer length results in the blue shift of the absorption wavelength, but the effect is less significant than for the dendronized version, namely, G2TTM (613 nm), G3TTM (598 nm), and G4TTM (584 nm) in toluene, respectively due to the larger delocalization in the dendrons that has more carbazole units.

PL spectra and PLQY (φ_f) of the radicals were recorded in cyclohexane (Table I, FIG. 2). Each radical in cyclohexane showed broad emission derived from the CT excited state, with emission maxima at 628 nm (Cz-TTM), 679 nm (BiCz-TTM), 675 nm (TriCz-TTM), and 662 nm (TetraCz-TTM). The excitation spectra in cyclohexane measured at the emission peak wavelengths agree well with the absorption spectra, indicating that the PL spectra originate from the radical (Fig. S19). The CT character of the excited state was confirmed by employing a toluene, more polar solvent than cyclohexane, where we found a red-shift of the emission wavelength and spectral broadening (Figs. S20). Substituent introduction of one carbazole unit into Cz-TTM resulted in a red shift of the emission wavelength by more than 50 nm and a significant decrease in PLQY, whereas further carbazole introduction resulted in a slight blue shift of the emission despite the increase of the carbazole oligomer HOMO level. A slight increase in PLQY (Cz-TTM: $\Phi_f = 89$ %; BiCz-TTM: $\Phi_f = 11$ %; TriCz-TTM: $\Phi_f = 16$ %; TetraCz-TTM: $\Phi_f = 24$ %) was also observed. This was similar to the behavior of carbazole dendronized radicals, but the degree of change in emission maxima and PLQY was smaller in oligomer-attached TTM radicals. Similar to the absorption, the PL spectra and PLQY showed a smaller but the same trend as the dendron-attached carbazole, suggesting that the carbazole oligomer-attached radicals show an effect of electron-electron repulsion of the occupied orbital on the donor, as do the carbazole dendrimer radicals.

FIG. 2

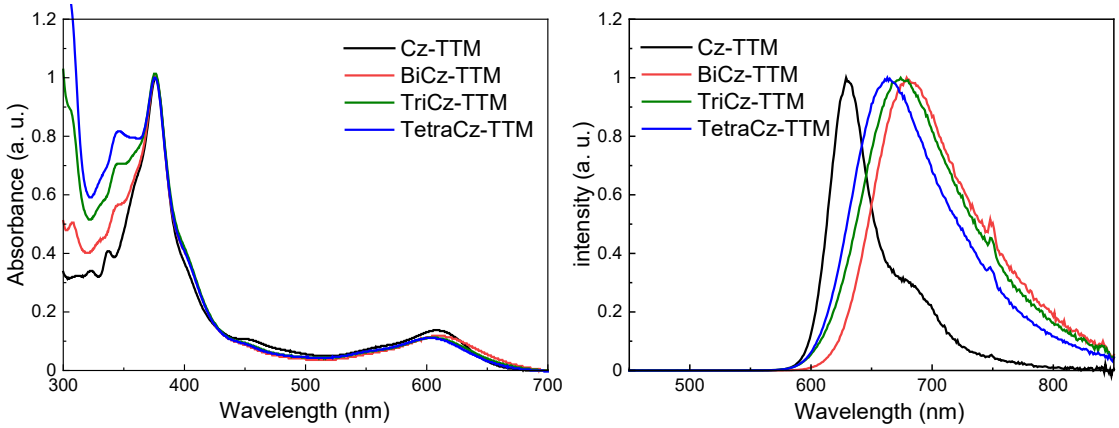

UV-Vis absorption spectrum (left) 10^{-5} M toluene and PL spectrum (right) of 10^{-5} M

cyclohexane.

To further understand the emission mechanism of oligomer-attached TTM radicals, the PL lifetime (τ) was measured. The PL lifetime curves in cyclohexane (Table I, FIG. 3) were fitted with a mono-exponential function and τ of 39.8 ns (Cz-TTM), 9.5 ns (BiCz-TTM), 14.2 ns (TriCz-TTM) and 17.5 ns (TetraCz-TTM) was obtained (Table I). From the PLQY and τ, the radiative rate constant (k_f) and the non-radiative rate constant (k_{nr}) were derived from the following equation 1 (Table I).

$$\varphi_f = \frac{k_f}{k_f + k_{nr}}, \tau = \frac{1}{k_f + k_{nr}} \qquad \text{equation 1}$$

The k_{nr} of BiCz-TTM (93.7×10^6 s) increased more than 30 times compared to Cz-TTM (2.8×10^6 s) and decreased as the oligomer length increased (TriCz-TTM: 59.2×10^6 s; TetraCz-TTM: 43.4×10^6 s). On the other hand, the k_f of oligomer-attached TTM radicals showed no significant change. The k_{nr} value of the oligomer-attached TTM radicals is strongly correlated with the emission maxima through the energy gap-law, i.e., the blue shift of the emission decreases the k_{nr}. A longer oligomer leads to blue shift of the emission due to the electron-electron repulsion effect and decreases the $k_{nr,}$ similar to the dendronized radicals.[24]

The photostability ($t_{1/2}$) of each radical was observed by monitoring the PL intensity during continuous irradiation with a 355 nm pulsed laser in cyclohexane (Table I, FIG. 4) The half-life was determined to be 6.8×10^1 s (TTM), 4.5×10^3 s (Cz-TTM), 1.7 10^4 s (BiCz-TTM), 9.8×10^3 s (TriCz-TTM) and 7.5×10^3 s (TetraCz-TTM), respectively. The photostabilities of the D-A type radicals were 60 times longer than that of the simple TTM radicals. Whereas the excited state of the simple TTM radical is a localized π-π* excited state, the oligomer-attached TTM radicals are a CT excited state, which may make photocyclization reactions at the TTM moiety more difficult. [26, 34] Although the detailed reasons are unclear, the inversely proportional relationship between photostability and τ for oligomer-attached TTM radicals suggests that their degradation process occurs at D_1 excited state.

FIG. 3

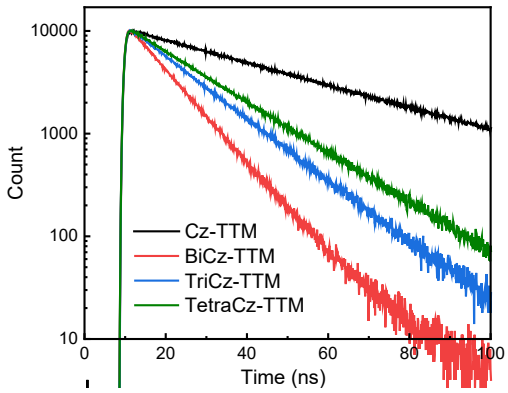

PL lifetime of Cz-TTM derivatives in cyclohexane.

FIG. 4

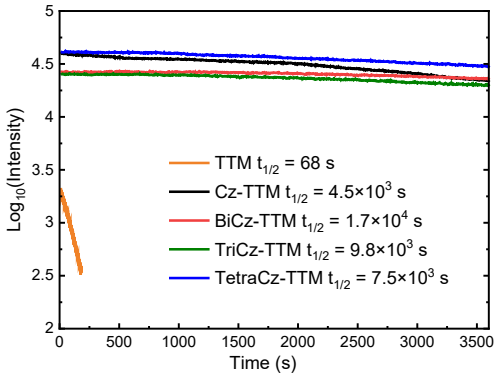

Time dependence of the emission intensity (I) for radicals in cyclohexane under 355 nm pulsed laser radiation (right), (power: 0.7 mW, beam diameter (1/e² level): ~3 mm, pulse width: 28 ps, repetition rate:10 Hz). The half-life ($t_{1/2}$) was determined by fitting the result with the equation $I(t) = I_0 \left(1/2\right)^{\frac{t}{t_{1/2}}}$ where $I(t)$ is the intensity at a specific time, I_0 is the initial intensity, and t is time.

Table I Photophysical properties of radicals.

Radical	λ_{Abs} (nm)[a]	λ_{PL} (nm)[b]	τ (ns)[b]	φ_f (%)[b]	k_f (10^6 s^{-1})	k_{nr} (10^6 s^{-1})	$t_{1/2}$ (10^3 s)[c]	ε (10^3 M^{-1} cm^{-1})[d]
Cz-TTM	609	628	39.8	89	22.4	2.8	4.5	3.7
BiCz-TTM	612	679	9.5	11	11.6	93.7	16.7	3.0
TriCz-TTM	605	675	14.2	16	11.3	59.2	9.8	3.0
TetraCz-TTM	603	662	17.5	24	13.7	43.4	7.5	2.9
G2TTM[e]	613	691	17.3	21	12.1	46.0	8.5	2.4
G3TTM[e]	598	663	48.8	52	10.7	9.8	2.8	3.1
G4TTM[e]	584	627	120.0	63	5.25	3.1	7.5	2.7

a) Absorption (λ_{Abs}) was measured in toluene solutions, b) PL (λ_{PL}), φ_f (PLQY), τ were measured in cyclohexane solutions (ca. 10^{-5} M), c) $t_{1/2}$ was measured absorbance of 0.5[-] at 355 nm in cyclohexane d) The molar absorption coefficient was measured in chloroform. e) Ref [24] $t_{1/2}$ was measured absorbance of 0.5[-] at 355 nm in toluene.

Density functional theory (DFT) calculations were performed to clarify the reason for the spectral blue shift with the length of carbazole units using Gaussian 16 Revision C.01.[35] The excited state electronic structures were computed at the TD-M06-2X/6-31G(d,p) level within the Tamm-Dancoff approximation. The DFT calculations using the M06-2X functional, compared with the B3LYP and CAM-B3LYP ones, have provided reasonable fluorescence spectra for the carbazole-dendronized radicals.[26] The solvent effect of cyclohexane was included through the polarizable continuum model. The effect of spin contamination in the unrestricted DFT calculations was minor (Table S2). The calculated fluorescence spectra, considering vibronic structures, well reproduced the experimentally observed blue shift from BiCz-TTM to Tetra-CzTTM (Fig. S21, see Ref.[36] for the computational details). The electron density difference of D_1-D_0 shows that D_1 is the intermolecular CT state (Fig. S22). The oligomeric carbazoles had an energetically high HOMO compared with the monomeric one (Fig. S23), resulting in larger D_1 dipole moments for the oligomer-attached TTM radicals than for Cz-TTM (Table S3). The increased CT character of the oligomer-attached TTM radicals smeared the vibronic progression in the fluorescence spectrum.

FIG. 5 shows the orbital levels of the oligomer-attached TTM radicals. The frontier orbital gap slightly decreased with the length of the carbazole units because of the HOMO shift to higher energy; the spectral blue shift observed from BiCz- to TetraCz-TTM cannot be explained by the one-electron picture. A previously proposed Hubbard model, represented by electron configurations comprising donor and acceptor fragment orbitals, shows that excitation energy increases when electron repulsion decreases in a donor unit while being constant in an acceptor unit (Fig. S24, see Supporting Information for the theoretical details).[26] The major configuration of D_1 was the βHOMO-βSUMO (SUMO; singly unoccupied molecular orbital) transition for BiCz- and TriCz-TTM and the βHOMO-1-βSUMO transition for TetraCz-TTM (Table S4). The occupied orbitals were more delocalized from BiCz-TTM to TetraCz-TTM across the entire donor unit, whereas the virtual orbitals were localized on the acceptor unit (see Table S5 for the quantification of the extent of delocalization [37, 38]). The value of electron repulsion was estimated from the two-electron integral over the molecular orbital comprising the major configuration of D_1, although the quantitative comparison between experiment and calculation requires consideration of other molecular orbital contributions. Additionally, the value was evaluated using CNDO/2 [39, 40] to simplify the computations, where the molecular orbitals calculated by CNDO/2 and DFT were similar (Fig. S25). The calculated electron repulsion for the occupied orbital decreased from BiCz-, TriCz-, and TetraCz-TTM and for the virtual orbital was similar (Table S5). Thus, the reduced electron repulsion in the donor unit, attributed to the greater orbital delocalization, was considered to induce the spectral blue shift.

A spectral blue shift with extended conjugation is also observed in donor-acceptor substituted oligomers.[41, 42] This is attributed to the diminishing CT character of the excited states. In fact, the D_1 dipole moment for the oligomer-attached TTM radicals decreased from BiCz- to TetraCz-TTM (Table

S3). Therefore, the small electron repulsion within the donor fragment can be regarded as a weak electron-donating ability.

The electron repulsion in the donor fragment for the oligomer-attached TTM radicals was larger than that for the dendron-attached ones when compared between the radicals with the same donor lengths (Table S6). For example, the values of BiCz- and G2TTM were calculated to be 0.2014 and 0.1717 a.u., respectively. This was because π-conjugation in the donor part of the oligomeric carbazoles was structurally confined at one side of the dendric parts of the dendrimers (see their chemical structures in Fig. 1). The electron felt a strong repulsion in the confined space. Thus, the blue shift utilizing the electron repulsion in the oligomer-attached TTM radicals was considered to be weakened compared to the dendron-attached ones. The control of electron repulsion through the length and number of attached donor units can allow for the delicate tuning of absorption and emission wavelengths. It is noted that the constructed Hubbard model for a donor-acceptor system cannot be applied to Cz-TTM because of the lessening CT character and, therefore, increasing the locally excited character compared with the oligomer-attached TTM radicals (Fig. S23 and Table S3). The spectral blue shift of Cz-TTM compared to other oligomer-attached radicals is attributed to the large frontier orbital gap.

FIG. 5

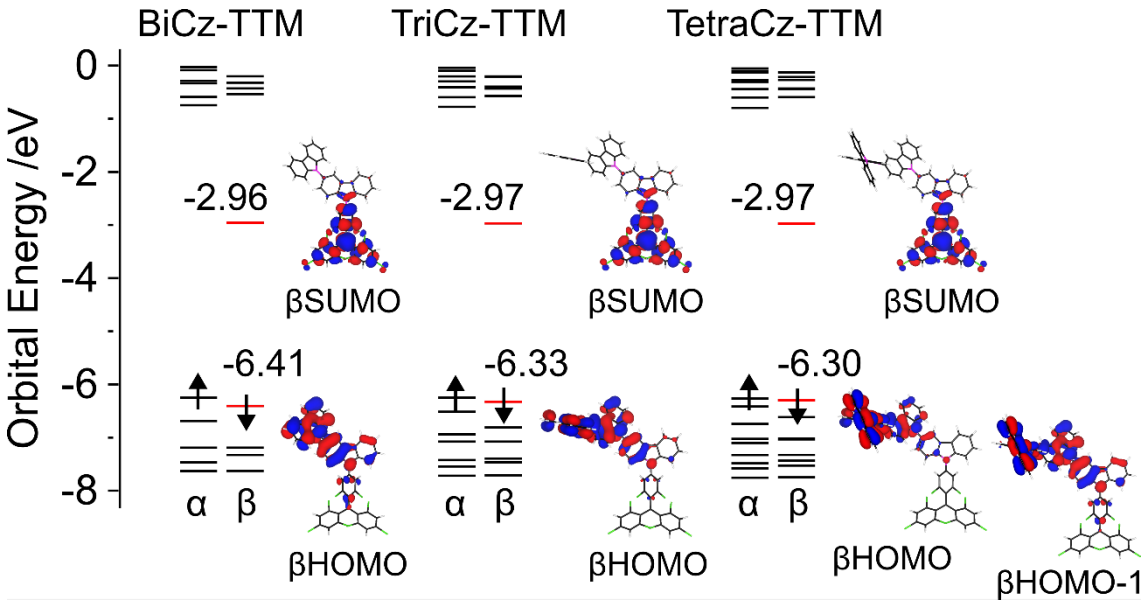

Calculated molecular orbital levels and molecular orbitals (isosurface value: 2×10^{-2} a.u.) at the D_1 optimized structure. Orbital energies of *β*HOMO and *β*SUMO are also shown.

FIG. 6

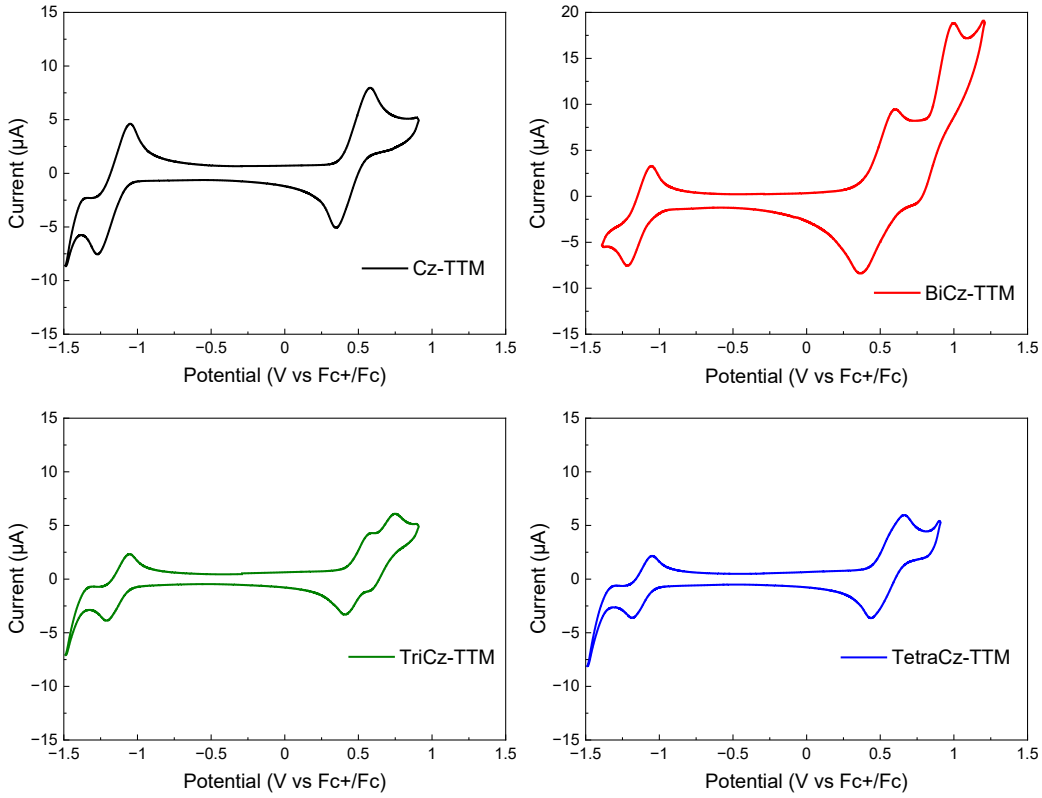

Cyclic voltammograms of Cz-TTM derivatives in 1 mM CH_2Cl_2 solution.

Cyclic voltammetry (CV) was measured to determine the redox potential and effect of the oligomeric carbazole moieties (FIG. 6, Figs. S26-S36). The results showed that the carbazole oligomer-substituted TTM radicals exhibited two or three reversible redox couples. The reduction/oxidation potentials ($E_{1/2}$) were -1.18/0.52 V vs Fc^+/Fc (Cz-TTM), -1.15/0.54/0.89 V (BiCz-TTM), -1.14/0.54/0.71 V (TriCz-TTM), and -1.14/0.54/0.59 V (TetraCz-TTM), respectively (FIG. 6 Figs. S26-S36). Redox couples around -1.18 to -1.14 V are reported to originate from the reduction of the TTM moiety and are largely independent of the donor structure.[19] The redox couple around 0.52-0.54 V is derived from the oxidation of the SOMO of the TTM moiety and was confirmed for all radical species. TTM acceptor-derived D-A radicals have been reported to form quinoid-like structures upon oxidation.[43, 44] Oxidation potentials were measured on the oligomeric carbazole donors alone to investigate the origin of the third redox couple at 0.89 V (BiCz-TTM), 0.71 V (TriCz-TTM) and 0.60 V (TetraCz-TTM) (Figs. S26-S36). The CV of the single donor showed an irreversible behavior derived from the electropolymerization behavior of carbazole, which makes it difficult to measure the exact potential (Figs. S26-S36).[45] The onset of the oxidation potentials were 0.89 V (BiCz), 0.73 V (TriCz), and 0.54 V (TetraCz), respectively, and we assumed that this onset trend reflects the HOMO level. Thus, the oxidation potentials of 0.89 V (BiCz-TTM), 0.71 V (TriCz-TTM) and 0.60 V (TetraCz-TTM) are

assigned to the oxidation of carbazole unit and are considered to have shifted to lower potentials with increasing the oligomer length due to extended conjugation of the oligomeric carbazoles. While cycling stability was low for TTM dendrimers, with electropolymerized carbazole-derived peaks becoming more pronounced after the second cycle, TTM radical species with linear oligomeric carbazoles showed reversible and stable cycling properties even after 10 cycles.[24]

III. CONCLUSION

In summary, carbazole oligomer-attached TTM radicals were synthesized and studied. As the carbazole oligomer length increased from 2 to 4, the absorption and emission were blue-shifted and the PLQY increased. The main reason for the increased PLQY is the suppression of non-radiative decay based on plausibly the larger energy gap. Theoretical calculations indicate that the blue shift with the increasing number of carbazoles stems from a decrease in electron-electron repulsion in the occupied orbitals on the oligomeric carbazoles, and the effect of electron-electron repulsion was shown to be smaller in the carbazole oligomer form compared to dendrimers. The introduction of oligomeric carbazoles significantly improved PLQY and photostability compared to TTM. It is noted that oligomer-attached TTM radicals exhibit more electrochemically stable redox properties than carbazole dendronized TTMs, indicating their potential for electro-optical conversion applications. Although a spectral blue shift can generally be achieved by shortening the conjugation and, therefore, expanding a frontier orbital energy gap, our strategy of utilizing electron-electron repulsion can give a blue shift even with extended conjugation. The utilization of electron-electron repulsion is confirmed as a new approach to tuning photophysical properties, such as emission maxima in luminescent radicals.

SUPPLEMENTARY MATERIAL

See the supplementary material for detailed experimental and calculation methods.

ACKNOWLEDGMENT

This work was supported, in part, by JSPS KAKENHI Grant No. JP23H02026, JP23H03966, and JP22K05253, JP24K23082, and the Cooperative Research Program of "Network Joint Research Center for Materials and Devices", and "Dynamic Alliance for Open Innovation Bridging Human, Environment and Materials" from MEXT, Japan. This study was also supported by the AIST Nanocharacterization Facility (ANCF) platform as a program of the "Nanotechnology Platform" (Grant Number JPMXP09A21AT0017) of MEXT, Japan. K. Albrcht thanks Transdisciplinary Energy Research (Q-PIT) through its "ModuleResearch" Program at Kyushu University. This work was supported by the Japan Science and Technology Agency (JST) as part of Adopting Sustainable Partnerships for Innovative Research Ecosystem (ASPIRE), Grant Number JPMJAP2334. K. Matsuda, and K. Anraku, thanks for the support from JST SPRING, Grant Number JPMJSP2136, and Grant-in-

Aid for JSPS Research Fellow Grant No. JP24KJ1764. Numerical calculations were partly performed at the Information Initiative Center, Hokkaido University.

AUTHOR DECLARATIONS

Conflict of Interest

The authors declare no competing financial interests.

Author Contributions

Kenshiro Matsuda: Conceptualization (supporting); Data curation (lead); Formal analysis (equal); Funding acquisition (supporting); Investigation (supporting); Methodology (supporting); Visualization (lead); Writing - original draft (lead); Writing - review & editing (supporting). **Wataru Ota:** Conceptualization (supporting); Data curation (equal); Formal analysis (equal); Investigation (equal); Methodology (equal); Resources (supporting); Visualization (equal); Writing - review & editing (equal). **Keiko Yamaoka:** Data curation (equal). **Kosuke Anraku:** Data curation (supporting); Formal analysis (supporting); Methodology (supporting). **Emiko Fujiwara:** Data curation (supporting); Formal analysis (supporting); Investigation (supporting). **Kazuhiro Nakamura:** Data curation (supporting); Investigation (supporting). **Takuya Hosokai:** Conceptualization (equal); Data curation (equal); Formal analysis (equal); Funding acquisition (equal); Investigation (equal); Resources (equal); Supervision (equal); Visualization (equal); Writing - review & editing (equal). **Tohru Sato:** Conceptualization (equal); Funding acquisition (equal); Investigation (equal); Methodology (equal); Project administration (equal); Resources (equal); Supervision (equal) Writing - review & editing (equal). **Ken Albrecht:** Conceptualization (equal); Funding acquisition (equal); Investigation (equal); Methodology (equal); Project administration (equal); Resources (equal); Supervision (equal); Writing - review & editing (equal).

DATA AVAILABILITY

The data that support the findings of this study are available from the corresponding author upon reasonable request.

REFERENCES

1 K. Nakamura, K. Matsuda, R. Xiaotian, M. Furukori, S. Miyata, T. Hosokai, K. Anraku, K. Nakao, K. Albrecht, *Faraday Discuss.,* 250, 192-201 (2024).

2 C. H. Liu, E. Hamzehpoor, Y. S. Otsuka, T. Jadhav, and D. F. Perepichka, *Angew. Chem., Int. Ed.,* 59(51), 23030-23034 (2020).

3 Y. Hattori, S. Kimura, T. Kusamoto, H. Maeda and H. Nishihara, *Chem. Commun.,* 54, 615-618 (2018).

4 X. Liu, C. Shi, M. Zhao, F. Li, J. Zhang, Z. Jiang, Q. Li, A. Yuan, and H. Yan, *Chem. Eur. J.,* 30(39), e202400927 (2024).

5 K. Tanushi, S. Kimura, T. Kusamoto, M. Tomonaga, Y. Kitagwa, M. Nakano, and H. Nishihara, *J. Phys. Chem. C,* 123(7), 4417-4423 (2019).

6 J. Ding, S. Dong, M. Zhang, and F. Li, *J. Mater. Chem. C,* 10, 14116-14121 (2022).

7 K. Lv, M. Zhang, and Feng Li, *J. Mater. Chem. C,* 11, 15892-15897 (2023).

8 F. Bejarano, I. J. O.-Contreras, A. Droghetti, I. Rungger, A. Rudnev, D. Gutierrez, M. M.-Torrent, J. Veciana, H. S. J. van der Zant, C. Rovira, E. Burzuri and N. Crivillers, *J. Am. Chem. Soc.*, 140(5), 1691-1696 (2018).

9 S. Kato, K. Ishizuki, D. Aoki, R. Goseki, and H. Otsuka, *ACS Macro Lett.,* 7(9), 1087-1091 (2018).

10 M. E. Arnold, L. Schoeneburg, M. Lamla, and A. J. C. Kuehne, *Molecules*, 29(5), 995 (2024).

11 X. Bai, W. Tan, A. Abdurahman, X. Li, and F. Li, *Dyes Pigm.,* 202, 110260 (2022).

12 S. Kimura, H. Nishihara, and T. Kusamoto, *Chem. Commun.*, 56, 11195-11198 (2020).

13 S. Kimura, M. Uejima, W. Ota, T. Sato, S. Kusaka, R. Matsuda, H. Nishihara, and T. Kusamoto, *J. Am. Chem. Soc.,* 143(11), 4329-4338 (2021).

14 S. Kimura, R. Matsuoka, S. Kimura, H. Nishihara, and T. Kusamoto, *J. Am. Chem. Soc.*, 143(15), 5610-5615 (2021).

15 X. Ai, E. W. Evans, S. Dong, A. J. Gillett, H. Guo, Y. Chen, T. J. H. Hele, R. H. Friend, and F. Li, *Nature*, 563, 536-540 (2018).

16 M. Ballester, J. Riera-Figueras and A. Rodríguez-Siurana, *Tetrahedron Lett.,* 11, 3615-3618 (1970).

17 O. Armet, J. Veciana, C. Rovira, J. Riera, J. Castaner, E. Molins, J. Rius, C. Miravitlles, S. Olivella, and J. Brichfeus, *J. Phys. Chem.,* 91(22), 5608-5616 (1987).

18 A. Abdurahman, T. J. H. Hele, Q. Gu, J. Zhang, Q. Peng, M. Zhang, R. H. Friend, F. Li, and E. W. Evans, *Nat. Mater.,* 19, 1224-1229 (2020).

19 K. Matsuda, R. Xiaotian, K. Nakamura, M. Furukori, T. Hosokai, K. Anraku, K. Nakao and K. Albrecht, *Chem. Commun.,* 58, 13443-13446 (2022).

20 A. Heckmann, S. Dümmler, J. Pauli, M. Margraf, J. Köhler, D. Stich, C. Lambert, I. Fischer, and U. Resch-Genger, *J. Phys. Chem. C,* 113(49), 20958-20966 (2009).

21 V. Gameroa, D. Velascob, S. Latorre, F. López-Calahorrab, E. Brillasc, and L. Juliá, *Tetrahedron Lett.,* 47**,** 2305-2309 (2006).

22 Q. Peng, A. Obolda, M. Zhang, and F. Li, *Angew. Chem., Int. Ed.*, 54(24), 7091-7095 (2015).

23 P. Ghosh, A. M. Alvertis, R. Chowdhury, P. Murto, A. J. Gillett, S. Dong, A. J. Sneyd, H.-H. Cho, E. W. Evans, B. Monserrat, F. Li, C. Schnedermann, H. Bronstein, R. H. Friend, and A. Rao, *Nature,* 629, 355-362 (2024).

24 R. Xiaotian, W. Ota, T. Sato, M. Furukori, Y. Nakayama, T. Hosokai, E. Hisamura, K. Nakamura, K. Matsuda, K. Nakao, A. P. Monkman, and K. Albrecht, *Angew. Chem., Int. Ed.,* 135(28), e202302550 (2023).

25 K. Albrecht, and K. Yamamoto, *J. Am. Chem. Soc.,* 131(6), 2244-2251 (2009).

26 S. Dong, A. Obolda, Q. Peng, Y. Zhang, S. Marder, and F. Li, *Mater. Chem. Front.,* 1, 2132-2135 (2017).

27 T. Xu, R. Lu, M. Jin, X. Qiu, P. Xue, C. Bao, and Y. Zhao, *Tetrahedron Lett.,* 46, 6883-6886 (2005).

28 T. Xu, R. Lu, X. Liu, P. Chen, X. Qiu, and Y. Zhao, *J. Org. Chem.,* 73(5), 1809-1817 (2008).

29 X. L. Liu, R. Lu, T. H. Xu, D. F. Xu, Y. Zhan, P. Chen, X. P. Qiu, and Y. Y. Zhao, *Eur. J. Org. Chem.,* 2009 (1), 53-60 (2009).

30 G. Xie, D. Chen, X. Li, X. Cai, Y. Li, D. Chen, K. Liu, Q. Zhang, Y. Cao, and S. Su, *ACS Appl. Mater. Interfaces,* 8(41), 27920-27930 (2016).

31 R. Yamada, K. Albrecht, T. Ohto, K. Minode, K. Yamamoto, and H. Tada, *Nanoscale,* 10, 19818-19824 (2018).

32 K. Albrecht, K. Matsuoka, K. Fujita, and K. Yamamoto, *Angew. Chem. Int. Ed.*, 54(19), 5677-5682 (2015).

33 A. Klapars, J. C. Antilla, X. Huang, and S. L. Buchwald, *J. Am. Chem. Soc.* 123(31), 7727-7729 (2001).

34 H. Guo, Q. Peng , X. Chen, Q. Gu, S. Dong, E. W. Evans, A. J. Gillett, X. Ai, M. Zhang, D. Credgington , V. Coropceanu, R. H. Friend, J. Brédas and F. Li, *Nat. Mater.,* 18, 977-984 (2019).

35 M. J. Frisch, G. W. Trucks, H. B. Schlegel, G. E. Scuseria, M. A. Robb, J. R. Cheeseman, G. Scalmani, V. Barone, G. A. Peterson, H. Nakatsuji, X. Li, M. Caricato, A. V. Marenich, J.

Bloino, B. G. Janesko, R. Gomperts, B. Mennucci, H. P. Hratchian, J. V. Ortiz, A. F. Izmaylov, J. L. Sonneberg, D. Williams-Young, F. Ding, F. Lipparini, F. Egidi, J. Goings, B. Peng, A. Petrone, T. Henderson, D. Ranasinghe, V. G. Zakrzewki, J. Gao, N. Rega, G. Zheng, W. Liang, M. Hada, M. Ehara, K. Toyota, R. Fukuda, J. Hasegawa, M. Ishida, T. Nakajima, Y. Honda, O. Kitao, H. Nakai, T. Vreven, K. Throssell, J. A. Montgomery Jr., J. E. Peralta, E. Ogliaro, B. Bearpark, H. J. J. E. Brothers, K. N. Kudin, V. N. Staroverov, T. Keith, R. Kobayashi, J. Normand, K. Raghavachari, A. Rendell, J. C. Burant, S. S. Iyengar, J. Tomasi, M. Cossi, J. M. Millam, M. Klene, C. Adamo, R. Cammi, J. W. Ochterski, R. L. Martin, K. Morokuma, O. Farkas, J. B. Foresman, D. J. Fox, Gaussian 16, Revision C. 01, Gaussian Inc., Wallingford, CT, 2019.

36 W. Ota, M. Uejima, and T. Sato, *Bull. Chem. Soc. Jpn.,* 96 (6), 582-590 (2023).

37 T. Lu and F. Chem, *J. Comput. Chem.* 33 (5), 580-592 (2012).

38 T. Lu, *J. Chem. Phys.* 161 (8), 082503 (2024).

39 J. A. Pople and G. A. Segal, *J. Chem. Phys.* 44 (9), 3289-3296 (1966).

40 D. P. Santry and G. A. Segal, *J. Chem. Phys.* 47 (1), 158-174 (1967).

41 H. Meier, J. Gerold, H. Kolshorn, B. Mühling, *Chem. Eur. J.,* 10 (2), 360–370 (2004).

42 H. Meier, *Angew. Chem. Int. Ed.,* 44 (17), 2482-2506 (2005).

43 J. F. Ambrose and R. F. Nelson , *J. Electrochem. Soc.,* 115, 1159 (1968).

44 A. Bobet, A. Cuadrado, L. Fajarí, I. Sirés, E. Brillas, M. P. Almajano, V. Jankauskas, D. Velasco, L. Juliá, *J. Phys. Org. Chem.* 32(9), e3974 (2019).

45 K. Karon and M. Lapkowski, *J. Solid State Electrochem.*, 19, 2601-2610 (2015).